

Article

Iberis sempervirens: Antiproliferative Potential from Our Garden

Azra Đulović ^{1,*} , Vedrana Čikeš Čulić ² , Franko Burčul ³  and Ivica Blažević ^{1,*} 

¹ Department of Organic Chemistry, Faculty of Chemistry and Technology, University of Split, Ruđera Boškovića 35, 21000 Split, Croatia

² School of Medicine, University of Split, Šoltanska 2, 21000 Split, Croatia; vedrana.cikes.culic@mefst.hr

³ Department of Analytical Chemistry, Faculty of Chemistry and Technology, University of Split, Ruđera Boškovića 35, 21000 Split, Croatia; franko@ktf-split.hr

* Correspondence: azra@ktf-split.hr (A.Đ.); blazevic@ktf-split.hr (I.B.)

Abstract: Glucosinolates (GSLs) extracted from various parts of *Iberis sempervirens* L., including seeds, stems, leaves, and flowers, were qualitatively and quantitatively assessed. The analyses of GSLs were performed by their desulfo counterparts using the UHPLC-DAD-MS/MS technique and by their volatile breakdown products, isothiocyanates, using the GC-MS technique. The GSL profile comprised various types, including those derived from: methionine, represented by methylsulfinylalkyl GSL (glucoiberin), and methylsulfonylalkyl GSL (glucoibervirin and glucoerucin); phenylalanine (glucotropaeolin); and tryptophan (4-methoxyglucobrassicin). Among these, the highest level of glucoiberin was detected in the leaves, reaching 35.37 $\mu\text{mol/g}$ of dry weight (DW), while the highest level of glucoibervirin was detected in the seeds, reaching 18.51 $\mu\text{mol/g}$ DW. To obtain GSL breakdown products, a variety of isolation methods were employed, including hydrodistillation in a Clevenger-type apparatus (HD), CH_2Cl_2 after myrosinase hydrolysis for 24 h (EXT), microwave-assisted distillation (MAD), and microwave hydrodiffusion and gravity (MHG). Volatile isolates were tested for their antiproliferative activity using an MTT assay against the human lung cancer cell line A549 and the human bladder cancer cell line T24 during an incubation period of 72 h. HD and MAD showed the best activity against T24, with IC_{50} values of 0.61 $\mu\text{g/mL}$ and 0.62 $\mu\text{g/mL}$, respectively, while EXT was the most effective against the A549 cell line, with an IC_{50} of 1.46 $\mu\text{g/mL}$.

Keywords: *Iberis sempervirens*; glucosinolates; isothiocyanates; antiproliferative activity; microwave-assisted isolation; A549 lung cancer cell line; T24 bladder cancer cell line



Citation: Đulović, A.; Čikeš Čulić, V.; Burčul, F.; Blažević, I. *Iberis sempervirens*: Antiproliferative Potential from Our Garden. *Appl. Sci.* **2024**, *14*, 346. <https://doi.org/10.3390/app14010346>

Academic Editor: Antony C. Calokerinos

Received: 9 October 2023

Revised: 18 December 2023

Accepted: 26 December 2023

Published: 29 December 2023



Copyright: © 2023 by the authors. Licensee MDPI, Basel, Switzerland. This article is an open access article distributed under the terms and conditions of the Creative Commons Attribution (CC BY) license (<https://creativecommons.org/licenses/by/4.0/>).

1. Introduction

The genus *Iberis* (Brassicaceae family) comprises ca. 30 species. The genus is primarily found in the Mediterranean basin, with Europe serving as its center of diversity. A few species are found in Northwest Africa, the Southwest, and Central Asia, and currently the genus has (nearly) a global distribution. However, several species have been imported outside of their native range [1,2]. Seven species and three more subspecies are growing wild in Croatia, one of which is *I. sempervirens* (evergreen candytuft) [3]. The name of the plant is derived from its Cretan and Spanish ancestry. While “candytuft” alludes to “the tufted plant from Candia”, which was the previous name for Crete, “*Iberis*” relates to Iberia, the Roman name for Spain. Although numerous phylogenetic studies have been undertaken to elucidate the evolutionary and taxonomic connections within the Brassicaceae family, it is worth noting that the genus *Iberis* was scarcely represented, typically consisting of just one or two species, in earlier investigations [4–8]. The *Iberis* species has not yet been the subject of thorough phylogenetic or phylogeographic research. According to the most recent phylogenetic studies, the placement of the *Iberis* genus alongside *Teesdalia* within the tribe Iberideae should be revisited by further taxonomic studies [4,9].

Considering the variability reported by Huang et al. (2020), the estimated age of the crown group of the Iberideae tribe was established at 14.6 ± 1.8 million years ago (mya) [10]. In the analyses of the *Iberis* species' tmrca, the most recent common ancestor is estimated to be older than 1 mya (ranging from 1.72 to 2.44 mya) [4].

Glucosinolates (GSLs) are plant-specialized metabolites found in Brassicaceae that include sulfur and nitrogen in their structures. GSLs first appeared around 92 mya, with arylaliphatic and branched GSLs originating from phenylalanine and branched chain amino acids (valine, isoleucine, and leucine), and indolic ones appearing around 77 mya originating from tryptophane. Met-derived GSLs emerged later, ca. 61 mya, and are associated with the Brassicaceae, Cleomaceae, and Capparaceae diversification [11–14].

GSLs are recognized as cancer prevention agents, biopesticides, and the source of distinctive flavor through the breakdown products they produce, mostly isothiocyanates (ITCs). To date, 90 of the 139 GSLs discovered in the plant kingdom have been fully characterized by modern spectroscopy techniques [15–17]. The distribution and level of the GSL identification in plants belonging to the *Iberis* genus investigated to date is given in the Table 1. Schultz and Gmelin in 1954 identified for the first time (*R*_S)-3-(methylsulfinyl)propyl GSL in *Iberis amara*, naming it glucoiberin (73) [18]. Later, (*R*_S)-3-(methylsulfonyl)propyl GSL was discovered by Kjær et al. (1955) in *I. sempervirens* and was named glucoibervirin (95) [19]. Several plants from the *Iberis* genus, including *I. amara*, *I. crenata*, *I. linifolia*, *I. sempervirens*, *I. simplex*, and *I. umbellata*, were mentioned in the earliest reports of the GSLs (prior to 2000). All the GSLs identified using paper chromatography and GC-MS analysis of breakdown products were Met-derived GSLs 73, 95, but-3-enyl GSL (gluconapin, 12), 3-(methylsulfonyl)propyl (glucocheirolin, 82), 4-(methylsulfonyl)butyl GSL (glucoerucin, 84), and prop-2-enyl GSL (sinigrin, 107).

Bennet et al. (2004) used the HPLC-MS technique to study the presence of GSLs in different plant seeds from the *Iberis* genus both qualitatively and quantitatively. They confirmed the presence of Met-derived GSLs as follows (from highest to lowest, respectively): *I. amara* (73, 95), *I. compacta* (82), *I. crenata* (82, 73), *I. gibraltarica* (73), *I. hybrida* (73), *I. saxatilis* (73), *I. sempervirens* (84, 95, 73, glucoraphanin (64), and 12), and *I. umbellata* (73, 107, 95) [20]. Using GC-MS, by their GSL breakdown products, namely but-3-enyl ITC, 4-(methylsulfonyl)butyl ITC and 5-(methylsulfonyl)pentanonitrile, 3-(methylsulfonyl)propyl ITC and 4-(methylsulfonyl)butanonitrile, and allyl ITC, Mastelić et al. also indicated the presence of GSL 12, 84, 95, and 107, respectively [21]. Using HPLC-MS and standards, Montaut et al. (2017) reported that *I. intermedia* seeds contain, next to Met-derived GSLs 73, 95, and 107, also Phe-derived GSL, i.e., benzyl GSL (glucotropaeolin, 11) [22]. Later report, using UHPLC-DAD-MS/MS and standards revealed in *I. umbellata* next to 12, 73, and 95, also Phe-derived GSL 11 and one Trp-derived 4-methoxyindol-3-ylmethyl GSL (4-methoxyglucobrassicin, 48) [23].

Table 1. Distribution of the glucosinolates in plants belonging to the *Iberis* genus investigated to date.

Species	Aminoacid Precursor									References
	Met							Phe	Trp	
	12	64	73	82	84	95	107	11	48	
<i>I. amara</i>			■		△	■				[18,20,24–27]
<i>I. compacta</i>				■						[20]
<i>I. crenata</i>	△		■	■						[20,26]
<i>I. gibraltarica</i>			■							[20]
<i>I. hybrida</i>			■							[20]
<i>I. intermedia</i>			▲			▲	▲	▲		[22]
<i>I. linifolia</i>			△	△						[26]

Table 1. Cont.

Species	Aminoacid Precursor									References
	Met							Phe	Trp	
	12	64	73	82	84	95	107	11	48	
<i>I. saxatilis</i>			■							[20]
<i>I. sempervirens</i>	■	■	■		■	■	△			[19–21,25]
<i>I. simplex</i>			△	△						[20]
<i>I. umbellata</i>	■		■			■	■	■	■	[20,23,26]

Benzyl GSL (glucotropaeolin, **11**), but-3-enyl GSL (gluconapin, **12**), 4-methoxyindol-3-ylmethyl GSL (4-methoxyglucobrassicin, **48**), 4-(methylsulfinyl)butyl GSL (glucoraphanin, **64**), 3-(methylsulfinyl)propyl GSL (glucoiberin, **73**), 3-(methylsulfonyl)propyl (glucocheirolin, **82**), 4-(methylsulfonyl)butyl GSL (glucoerucin, **84**), 3-(methylsulfonyl)propyl GSL (glucoibervirin, **95**), and prop-2-enyl GSL (sinigrin, **107**). △: “Circumstantial evidence”—reasonable, but not conclusive evidence of qualitative analysis; ▲: “Present”—qualitative analysis performed by using one or more relevant analysis methods (using standards, MS, and/or NMR); ■: Qualitative and quantitative analysis performed.

Liu et al. (2019) isolated essential oil from *Iberis amara* seeds using various methods, including steam distillation, hydrodistillation, and ultrasound-assisted hydrodistillation. They have identified certain volatile compounds, specifically but-3-enyl ITC, 3-methylbutyl ITC, and butyl ITC. However, these compounds were not included in Table 1 because no standards were employed for their identification. They have tested the obtained volatile isolates for their cytotoxic effects on human colon cancer cell lines SW480 and HCT116, revealing inhibitory concentrations (IC₅₀) in the range of 35–42 µg/mL and 63–70 µg/mL, respectively [28]. The hydroethanolic *I. amara* extract, a popular phytomedicine for treating digestive problems, dramatically reduced the growth of HT-29 and T84 colon carcinoma cells, having IC₅₀ values of 6 and 9 µg/mL, respectively.

The researchers also conducted experiments on two different cancer cell models, specifically PC-3 prostate cancer cells and MCF7 breast cancer cells. Similar to the previous findings for the two colon cancer models, the *I. amara* extract exhibited an inhibitory effect on the proliferation of PC-3 and MCF7 cancer cells, with IC₅₀ values of 44 g/mL and 11 g/mL, respectively.

In the case of HT-29 cells, the inhibition of cell proliferation was accompanied by the arrest of the cell cycle in the G2/M phase and a reduction in the expression of several regulatory marker proteins. Importantly, the *I. amara* extract promoted apoptosis in HT-29 cells by inducing the intracellular production of reactive oxygen species. Furthermore, when administered orally at a dosage of 50 mg/kg twice a day for a duration of 4 weeks, the *I. amara* extract significantly suppressed tumor growth in a mouse HT-29 tumor xenograft model. These results are consistent with predictions from in vitro research [29].

The primary objective of this research was to detect and quantify GSLs in various parts of the wild-growing *I. sempervirens* plant by analyzing their desulfo counterparts through the use of UHPLC-DAD-MS/MS. Additionally, the study involved the analysis of the volatile isolates obtained from *I. sempervirens* using different methods: hydrodistillation, CH₂Cl₂ extraction after a 24-h autolysis period, and microwave-assisted isolation (comprising microwave distillation, microwave hydrodiffusion, and gravity). Furthermore, the antiproliferative activity of the obtained isolates was tested against two human cancer cell lines, specifically lung A549 and bladder T24, using the MTT method.

2. Materials and Methods

2.1. General

DesulfoGSLs were analyzed using UHPLC-DAD-MS/MS (Ultimate 3000RS with TSQ Quantis MS/MS detector, Thermo Fisher Scientific, Waltham, MA, USA) and a Hypersil

GOLD C18 column (100 × 3.0 mm, 3.0 µm, Thermo Fisher Scientific, Waltham, MA, USA), while the volatiles were analyzed using GC-MS (consisting of model 8890 GC, automatic liquid injector, model 7693A and a tandem mass spectrometer, model 7000D GC/TQ, Agilent Inc., Santa Clara, CA, USA), and a non-polar HP-5MS UI column (30 m × 0.25 mm, 0.25 µm, Agilent Inc., Santa Clara, CA, USA). Hydrodistillation (HD) was performed in Clevenger-type apparatus (Deotto Lab, Zagreb, Croatia), whereas microwave-assisted isolation was performed in ETHOS X (Milestone Inc., Bergamo, Italy). A microplate photometer (model HiPo MPP-96, BioSan, Riga, Latvia) was used for the MTT spectrophotometric test.

2.2. Plant Material

The *Iberis sempervirens* L. sample (seed, stem, leaf, and flower) was obtained from wild-growing plants collected in Podstrana (Split, 43°70'36" N, 16°57'41" E) in May 2019. A local botanist, Dr. Mirko Ruščić, from the Faculty of Natural Sciences, University of Split, Croatia, confirmed the botanical identity of the plant material, which is stored under voucher number ZOKISP1.

2.3. Chemicals and Reagents

Myrosinase, sulfatase, sinigrin, allyl ITC, 3-(methylsulfanyl)propyl ITC, and 3-(methylsulfinyl)propyl ITC were obtained from Sigma Aldrich (St. Louis, MO, USA). Benzyl GSL (glucotropaeolin, **11**), 4-methoxyindol-3-ylmethyl GSL (4-methoxyglucobrassicin, **48**), and 4-(methylsulfanyl)butyl GSL (glucoerucin, **84**) were obtained from Phytoflan (Heidelberg, Germany). 3-(Methylsulfinyl)propyl GSL (glucoiberin, **73**) was isolated from *Anastatica hierochuntica* in its desulfo-form and confirmed by NMR. All other chemicals and reagents were of analytical grade. Human cancer cell lines (lung A549 and bladder T24) were obtained from the American Type Tissue Culture Collection (ATCC, Manassas, VA, USA) and cultured in a humidified atmosphere with 5% CO₂ at 37 °C in Dulbecco's modified Eagle medium (DMEM, EuroClone, Milan, Italy) containing 4.5 g/L glucose, 10% fetal bovine serum (FBS), and 1% antibiotics (Penicillin Streptomycin, EuroClone, Milan, Italy).

2.4. Isolation and Chemical Analysis

2.4.1. Isolation of Desulfoglucosinolates

GSLs were isolated as previously reported [14]. Different plant parts (seed, stem, leaf, and flower, 100 mg) were extracted twice in 1 mL of boiling MeOH–H₂O (7:3). The extracted GSLs were then bound to anion exchange mini columns filled with 0.5 mL of DEAE-Sephadex A-25 (GE Healthcare, Chicago, IL, USA). The columns were washed with 70% MeOH (2 mL) and ultrapure water (1 mL), and sodium acetate (25 mM) was used for conditioning. Each mini-column was loaded with purified sulfatase (20 µL; 0.35 U/mL) and left to stand for 18 h at room temperature. The obtained desulfoGSLs were then eluted with ultra-pure H₂O (1.5 mL), lyophilized, and dissolved in ultra-pure water (1 mL). The samples were stored at –20 °C until further analysis by UHPLC-DAD-MS/MS.

2.4.2. UHPLC-DAD-MS/MS Analysis

A gradient of solvents A (50 µM NaCl in H₂O) and B (acetonitrile:H₂O 30:70 v/v) was applied at a flow rate of 0.5 mL/min as follows: 0.14 min 96% A; 7.84 min 14% A; 8.96 min 14% A; 9.52 min 5%; 13.16 min 5% A; 13.44 min 96% A; 15.68 min 96% A. The injection volume was 5 µL, and the oven temperature was kept at 25 °C. The mass spectrometer was run with positive electrospray ionization (H-ESI source). The capillary voltage was 3500 V at 350 °C. GSLs were recorded at λ = 227 nm and quantified using a calibration curve of desulfosinigrin (ranging from 0.14 to 1.4 mM) and relative response factors for each individual desulfoGSL as follows: 0.95 for **11**, 0.25 for **48**, 1.07 for **73**, 1.04 for **84**, and 0.80 for **95** [30].

2.4.3. Isolation of Volatiles

Different methods, as previously described [31], were used to isolate volatiles. The first method, hydrodistillation (HD) in the Clevenger apparatus, was carried out using the whole plant material (seed, stem, leaf, and flower, 50 g) for 2.5 h. In the second approach, the whole plant material (seed, stem, leaf, and flower, 10 g) was immersed in water (50 mL) with the addition of myrosinase (1–2 units) and left to hydrolyze for 24 h at 27 ± 2 °C. Volatiles were subsequently extracted by CH_2Cl_2 (EXT). Additional modern methods included microwave-assisted isolation, microwave-assisted distillation (MAD), and microwave hydrodiffusion and gravity (MHG). MAD was conducted using fresh plant material (100 g) for 35 min at 500 W. The distillate was concentrated in a pentane trap. In the case of MHG, the isolation process was shortened to 15 min with the same power applied. The aqueous extract was gathered, and the volatile components were extracted using dichloromethane (CH_2Cl_2). Afterward, the extract was dried using anhydrous sodium sulfate and concentrated using an automated sample concentrator (VLM GmbH, Bielefeld, Germany). All samples were stored at -20 °C until the GC-MS analysis.

2.4.4. GC-MS Analysis

The column temperature program was the following: 60 °C for 3 min, heated to 246 °C at 3 °C/min, and maintained at that temperature isothermally for 25 min. The flow rate of helium carrier gas was 1 mL/min. The volume of the injected sample was 1 μL , and the inlet temperature was 250 °C. The quadrupole temperature was set to 150 °C, the ion source temperature was 230 °C, and the ionization energy was 70 eV. The analyses were carried out in duplicate.

To identify individual peaks, their Kovats retention indices were compared to those in the literature and/or authentic samples, and their mass spectra were compared to those in the Wiley 9N08 MS (Wiley, New York, NY, USA) and NIST17 (Gaithersburg, MD, USA) databases.

2.5. Cell Viability Assay (MTT)

The cells (human lung cancer cell line A549 and bladder cancer cell line T24) were treated with the volatile isolates (HD, MAD, EXT, and MHG) at concentrations of 1, 5, 10, 50, and 100 $\mu\text{g/mL}$ (in DMSO) in a complete medium (in triplicate) for 72 h, as previously described [31]. The media was removed after the cells had been treated with 0.5 g MTT/L for 2 h at 37 °C. DMSO was then added, and the mixture was incubated for an additional 10 min at 37 °C while being shaken. The degree of formazan formation, an indicator of living and metabolically active cells, was measured at 570 nm. The results were compared to the untreated control group (DMSO with no volatile isolates added, 100% viability) using three different experiments. Cisplatin (50 $\mu\text{g/mL}$) was used as the positive control. GraphPad Prism software, version 7.0, was used to calculate the IC_{50} values as well as perform statistical analyses using *t*-test with unequal variances. Based on IC_{50} values, the following criteria were used to classify the activity against the investigated cell lines: ≤ 20 $\mu\text{g/mL}$ = highly active, 21–200 $\mu\text{g/mL}$ = moderately active, 201–500 $\mu\text{g/mL}$ = weakly active, and ≥ 501 $\mu\text{g/mL}$ = inactive [32].

3. Results and Discussion

3.1. Glucosinolates and Volatiles

UHPLC-DAD-MS/MS analysis of *I. sempervirens* revealed the presence of five (5) desulfoGSLs, dominated by GSLs derived from methionine (homoMet) and chain elongated methionine (dihomoMet), but also contained GSLs derived from Phe and Trp (Table 2, Figures 1 and S1). The main GSLs originating from methionine biosynthesis with chain lengths C3–C4 were 3-(methylsulfinyl)propyl GSL (glucoiberin, 73), 3-(methylsulfonyl)propyl GSL (glucoibervirin, 95), and 4-(methylsulfonyl)butyl GSL (glucoerucin, 84). Benzyl GSL (glucotropaeolin, 11) was the only arylaliphatic GSL identified, while 4-methoxyindol-3-

ylmethyl GSL (4-methoxyglucobrassicin, **48**) was the only indolic type GSL; both were present in traces.

Table 2. Glucosinolate content in *Iberis sempervirens*.

No. *	Glucosinolate (GSL) (Trivial Name)	t_R (min)	$[M + Na]^+$	Glucosinolate Content ($\mu\text{mol/g DW}$)			
				Seed	Stem	Leaf	Flower
73	HomoMet-derived 3-(Methylsulfinyl)propyl GSL (glucoiberin)	1.14	366	5.52 ± 0.21	6.94 ± 0.09	35.37 ± 1.13	19.76 ± 0.97
95	3-(Methylsulfonyl)propyl GSL (glucoibervirin)	5.50	350	18.51 ± 0.18	11.20 ± 0.54	1.12 ± 0.07	2.88 ± 0.10
84	DihomoMet-derived 4-(Methylsulfonyl)butyl GSL (glucoerucin)	6.40	364	tr	tr	n.d.	n.d.
11	Phe-derived Benzyl GSL (glucotropaeolin)	6.50	352	n.d.	tr	n.d.	tr
48	Trp-derived 4-Methoxyindol-3-ylmethyl GSL (4-methoxyglucobrassicin)	8.02	421	n.d.	tr	tr	n.d.
Total ($\mu\text{mol/g DW}$)				24.03 ± 0.39	18.14 ± 0.63	36.49 ± 1.20	22.64 ± 1.07

* No.—numbers are related to the glucosinolate number given in the review paper by Blažević et al. [15], and the structures are shown in Figure 1. All chromatograms are given in Figure S1, while MS² spectra are given in Figure S2. DW—dry weight; tr—traces < 0.01 $\mu\text{mol/g DW}$; n.d.—not detected. The data are expressed as the mean value \pm standard error ($n = 3$). homo—the higher homologue of a specified amino acid.

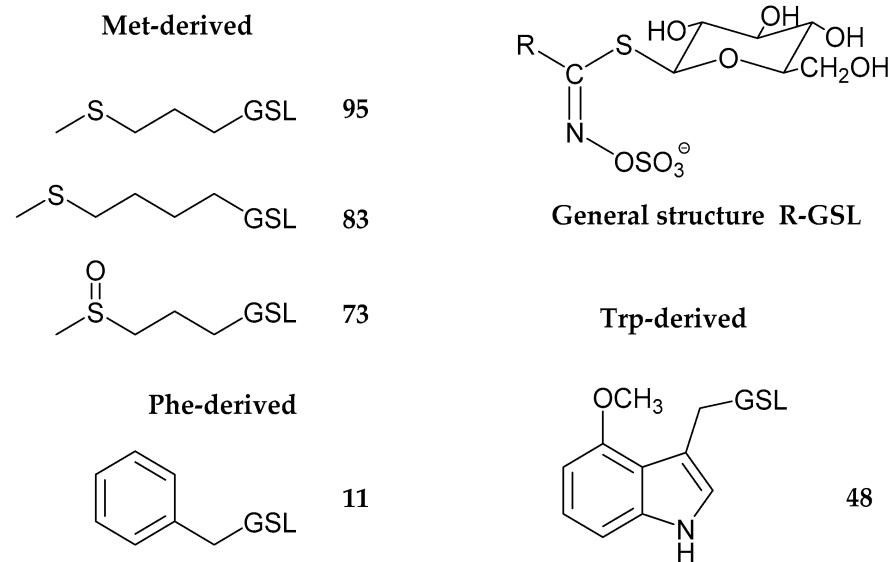


Figure 1. Structures of the GSLs identified in *Iberis sempervirens* (see Table 1).

Identification of desulfoGSLs was based on their m/z values and retention times, as well as the MS² spectra that contained the fragments, which enabled the confirmation of the structures identified (Figure S2). The MS² spectrum of methylsulfinylalkyl dGSL **d73** showed the fragment m/z 302 from a neutral loss of CH_3SOH from the sodium adduct, while the MS² spectrum of methylsulfonyl analogue **d95** showed only fragments of sodium adducts with anhydroglucose and thioglucose due to the low polarity of the side chain. Additionally, the fragment formed by the loss of oxidized thioglucose (m/z 212) that is characteristic of this type of dGSL was also observed for **d95** [33].

The more lipophilic 3-(methylsulfanyl)propyl GSL **95** was the major GSL in seeds (18.51 $\mu\text{mol/g}$ DW) and stems (11.20 $\mu\text{mol/g}$ DW). Traces of the higher C4 homologue, GSL **84**, were also detected in the same plant parts. GSL **73**, the oxidized form of **95**, was found at the highest level in the leaves of *I. sempervirens*, with 35.37 $\mu\text{mol/g}$ of DW, followed by 19.76 $\mu\text{mol/g}$ of DW in the flowers. Phe-derived GSL **11** was identified in this species for the first time, as was Trp-derived GSL **48**. These types of GSLs found at low levels are not ubiquitous for the *Iberis* genus (Table 1). The *Iberis* genus appears to be limited to the biosynthesis of C3 and C4 GSLs derived from homoMet and dihoMet amino acids (Table 1), which is consistent with the occurrence of GSLs derived from n-homoMet as well as from Phe and Trp in the Brassicaceae family [13].

Indirect analysis of GSLs via their degradation products was also performed. Myrosinase, both endogenous and exogenous, degraded GSLs enzymatically during the autolysis for 24 h, while thermal degradation was assessed using conventional (hydrodistillation, HD) and modern (microwave-assisted distillation, MAD; and microwave hydrodiffusion and gravity, MHG) techniques. The volatile isolates obtained from whole plant material were analyzed by GC-MS (Table 3).

Table 3. Volatiles obtained from the whole plant of *Iberis sempervirens* using different methods of isolation.

No. *	Parent Glucosinolate Identified Breakdown Compound	KI	HD (%)	MAD (%)	EXT (%)	MHG (%)
95	Glucoibervirin					
	4-(Methylsulfanyl)butanenitrile ^b	1083	n.d.	n.d.	n.d.	37.31
	3-(Methylsulfanyl)propyl isothiocyanate ^{a,b}	1308	99.90	99.11	1.72	60.05
73	Glucoiberin					
	Allyl isothiocyanate ^{a,b,c}	890	tr	n.d.	58.61	n.d.
	3-(Methylsulfanyl)propyl isothiocyanate ^{a,b}	1745	n.d.	n.d.	27.05	n.d.
Other volatiles						
	(Z)-Hex-2-enal ^b	826	n.d.	n.d.	7.01	n.d.
	S-methyl methanethiosulfinate ^b	990	tr	n.d.	tr	n.d.
	Nonanal ^b	1105	tr	tr	n.d.	n.d.
	Diethyl phthalate ^b	1618	n.d.	n.d.	5.00	1.03
Total (%)			99.90	99.11	99.39	98.39
Yield ($\mu\text{g/g}$)			243.03	137.23	40.36	51.49

* No.—numbers are related to the glucosinolate number given in the review paper by Blažević et al. [15]. HD—hydrodistillate; MAD—microwave-assisted distillate; EXT—CH₂Cl₂ extract after the 24 h autolysis with added myrosinase; MHG—extract obtained by microwave hydrodiffusion and gravity; KI—Kovats retention indices determined on a HP-5MS UI capillary column; n.d.—not detected, tr—traces. The percentages represent the average component percentages obtained from duplicate analyses on the HP-5MS UI column. ^a Compound identified by mass spectra and KI comparison with a standard. ^b Compound identified by mass spectra comparison with the Wiley/NIST library. ^c This compound is the thermolysis product of 3-(methylsulfanyl)propyl ITC during GC-MS analysis (Figure 2).

Sulfur-containing volatiles found in the analyzed samples differed depending on the method used for their isolation. Hydrodistillate and microwave distillate contained only one GSL degradation product, 3-(methylsulfanyl)propyl ITC, originating from **95**. On the other hand, three ITCs were identified in the dichloromethane extract with the highest percentage of allyl ITC (58.61%). Also, this was the only volatile isolate that contained 3-(methylsulfanyl)propyl ITC (iberin) derived from the main GSL **73** (28.2%), but with the lowest percentage of sulfanyl analogue (1.72%) among all isolates. Allyl ITC is an olefinic ITC derived from sinigrin (**107**) that was not detected by dGSL analysis (searched but not found), which is why it was concluded to be an artifact arising from the present methylsulfanyl ITC during GC-MS measurements (Figure 2).

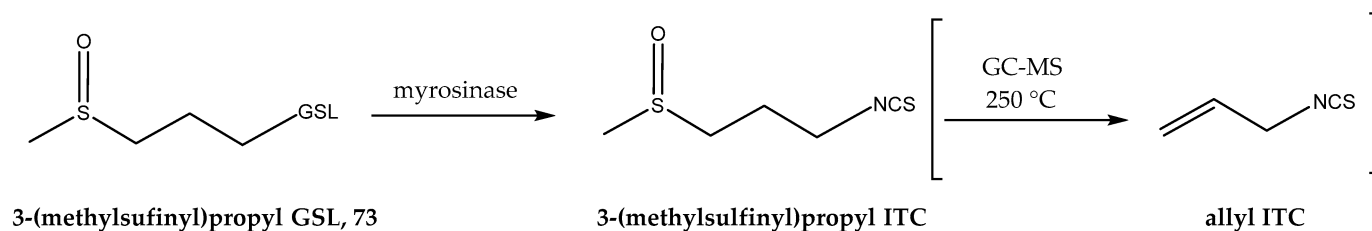


Figure 2. Degradation of 3-(methylsulfinyl)propyl GSL (73) to corresponding methylsulfinylalkyl isothiocyanate (ITC) and his thermolysis product during GC-MS analysis (detected in the autolysis volatile).

This was also observed in the case of GC-MS analyses of *Lunaria annua* L. volatiles. Two alkenyl ITCs, pent-4-enyl ITC and hex-5-enyl ITC, were identified in the EXT and MHG, with no such alkenyl dGSLs identified by UHPLC-MS/MS analysis. It was concluded that these ITCs were formed due to the thermolysis of corresponding ω -(methylsulfinyl)alkyl ITCs, 5-(methylsulfinyl)pentyl ITC, and 6-(methylsulfinyl)hexyl ITC during GC-MS analysis [31]. Using only an indirect method to identify GSLs might be misleading, and the allyl ITC formation observed in this study is another cautionary example. Furthermore, in the case of previously investigated *I. sempervirens* and *I. crenata* (Table 1), the identification of olefinic GSLs singirin (107) and gluconapin (12), respectively, based solely on the indirect GC-MS analysis strongly suggests that these GSLs are absent and are instead artifacts arising from the thermolysis of the corresponding ω -(methylsulfinyl)alkyl ITCs.

Microwave hydrodiffusion and gravity resulted in the formation of two degradation products: methylsulfonyl GSL 95, 3-(methylsulfonyl)propyl ITC (59.0%), and the corresponding nitrile (36.3%). By comparing the GSL profile with the identified degradation products, it was concluded that methylsulfonylalkyl GSL 95 is degraded under microwave-assisted thermal decomposition conditions, while its oxidized methylsulfinyl form 73 is stable under the same conditions. This observation is supported by the fact that the MAD volatile isolate contained only a degradation product of 95 as well (Table 3).

3.2. Antiproliferative Activity

Hydrodistillate (HD), CH_2Cl_2 extract following autolysis (EXT), as well as isolates obtained through microwave hydrodiffusion and gravity (MHG) and microwave distillation (MAD), were evaluated for their antiproliferative activity against the human lung cancer cell line A549 and the human bladder cancer cell line T24 (Figure 3, Table 4).

EXT can be considered highly active on both cell lines, with an IC_{50} of 1.46 $\mu\text{g/mL}$ for the A549 cell line and 1.83 $\mu\text{g/mL}$ for the T24 cell line achieved after 72 h of incubation. These high antiproliferative activities of EXT can be attributed to the presence of 3-(methylsulfinyl)propyl ITC (identified as 3-(methylsulfinyl)propyl ITC and allyl ITC comprising over 85% of total volatiles (Table 3, Figure 2). Samples obtained by HD and MAD, both containing more than 99% of 3-(methylsulfonyl)propyl ITC (Table 2), displayed comparably high activity with IC_{50} values of 8.45 $\mu\text{g/mL}$ and 9.42 $\mu\text{g/mL}$ for A549 and 0.61 $\mu\text{g/mL}$ and 0.62 $\mu\text{g/mL}$ for T24 cell lines, respectively. On the other hand, MHG exhibited slightly lower activity on both cell lines compared to the other isolates and was the only isolate containing 4-(methylsulfonyl)butanenitrile (37%), along with the corresponding ITC (60%).

Previously, volatile isolates of different plants containing ITCs were tested against these two cell lines: bladder T24 (*Armoracia rusticana*, *Sysimbrium officinale*) and lung A549 (*A. rusticana*, *Lunaria annua*, *S. officinale*, *Lobularia lybica*) [14,31,32,34]. The major ITCs found in these volatile isolates can be categorized into arylaliphatic and aliphatic (olefinic, branched, and/or sulfur-containing) types. Volatile isolates from *A. rusticana* containing 2-phenylethyl ITC and allyl ITC as the major constituents as well as the tested standards showed high activity against the T24 cancer cell line, while isopropyl ITC, as the major volatile in *S. officinale*, had moderate activity [14,34]. High activities against

the A549 cancer cell line were observed for volatile isolates from *A. rusticana* (containing 2-phenylethyl ITC and allyl ITC) and for volatile isolates from *L. annua* (containing 5-(methylsulfinyl)pentyl ITC and 6-(methylsulfinyl)hexyl ITC). On the other hand, the isolates containing isopropyl ITC (from *L. annua* and *S. officinale*) and 3-(methylsulfonyl)propyl ITC (from *L. lybica*), as the major ones, had moderate to low activity for the same cell line [14,32,33,35]. The difference in antiproliferative activity against the A549 cell line of the ITCs with different oxidation states of sulfur atoms in the side chain was also observed by Wang et al. They showed that the factor in ITCs' cytotoxicity is associated with the negative charge populations, delocalization of the border molecular orbital, and energy gaps of the HOMO-LUMO [35]. Since the charge of the oxygen atom is more negative than the charge of the sulfur atom, the cytotoxicity of 4-(methylsulfinyl)butyl ITC (sulforaphane) and 3-(methylsulfinyl)propyl ITC was higher than that of 3-(methylsulfonyl)propyl ITC. The A549 cells treated with 3-(methylsulfonyl)propyl ITC and 3-(methylsulfinyl)propyl ITC displayed typical morphological signs of apoptosis, with 3-(methylsulfinyl)propyl ITC generating higher rates of cellular apoptosis than 3-(methylsulfonyl)propyl ITC [35].

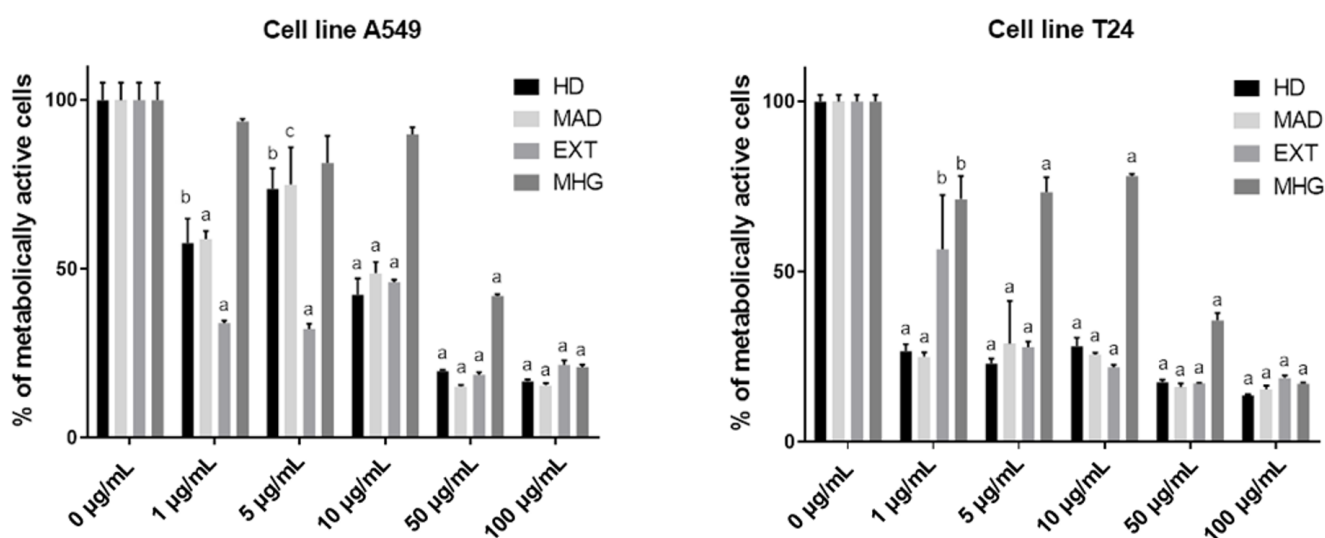


Figure 3. Percentage of metabolically active cells in human lung cell line A549 and human bladder cell line T24 after 72 h of incubation with different concentrations of *I. sempervirens* samples. HD—hydrodistillate; MAD—microwave-assisted distillate; EXT—CH₂Cl₂ extract after the 24 h autolysis with added myrosinase; MHG—extract obtained by microwave hydrodiffusion and gravity. Calculated IC₅₀ values (µg/mL) are given in Table 4. Each data point is presented as the mean ± SD (n = 3). Lowercase letters represent the significance level in comparison to non-treated cell line samples (a, $p < 0.001$; b, $p < 0.01$; c, $p < 0.05$).

Table 4. Calculated IC₅₀ values (µg/mL) for volatiles obtained by HD, MAD, EXT, and MHG from the whole plant material (seed, stem, leaf, and flower) against human lung cancer cell A549 and bladder cancer cell T24 lines after 72 h.

Cell Line	IC ₅₀ (µg/mL)				Control ^a
	HD	MAD	EXT	MHG	
A549	8.45	9.42	1.46	36.41	84.71%
T24	0.61	0.62	1.83	23.30	52.32%

HD—hydrodistillate; MAD—microwave-assisted distillate; EXT—CH₂Cl₂ extract after the 24-h autolysis with added myrosinase; MHG—extract obtained by microwave hydrodiffusion and gravity. ^a The percentages of metabolically active cells (as % total cells) for cisplatin as a positive control (50 µg/mL) after 72 h.

4. Conclusions

Throughout history, *Iberis* species have been researched for the presence of GSLs using various approaches. These studies revealed that they primarily contain GSLs derived from

methionine. This was supported by phylogenetic studies that link the evolution of both the Brassicaceae family and the related GSLs. However, some of the research on these plant species was carried out by utilizing indirect methods of GSL identification, i.e., GC-MS analyses of their breakdown products. This and other studies suggest that some former findings should be re-evaluated using suitable spectroscopic techniques for direct GSL identification. GSL breakdown products, usually ITCs, are mostly associated with the observed bioactive properties, as opposed to the other volatiles that can be formed, such as nitriles. This work underlines the significance of adopting appropriate conditions for GSL degradation (thermal or enzymatic) as well as the selection of the method used for isolation, such as distillation or extraction, due to the differences in polarity and molecular weight. It is also evident that the oxidation state of the sulfur in the side chain, next to the ITC functional group, influences the bioactivity potential as well.

Supplementary Materials: The following supporting information can be downloaded at: <https://www.mdpi.com/article/10.3390/app14010346/s1>, Figure S1: Chromatograms of desulfoglucosinolates (dGSLs) obtained from the different plant parts of *I. sempervirens*. **d73**—3-(methylsulfinyl)propyl dGSL (desulfoglucosinoin); **d95**—3-(methylsulfinyl)propyl dGSL (desulfoglucosinoin); **d84**—4-(methylsulfinyl)butyl dGSL (desulfoglucosinoin); **d11**—benzyl dGSL (desulfoglucosinoin); **d48**—4-methoxyindol-3-ylmethyl dGSL (desulfo-4-methoxyglucobrassicin); Figure S2: MS² spectra of desulfoglucosinolates from *I. sempervirens*. **d73**—3-(methylsulfinyl)propyl dGSL (desulfoglucosinoin); **d95**—3-(methylsulfinyl)propyl dGSL (desulfoglucosinoin); **d84**—4-(methylsulfinyl)butyl dGSL (desulfoglucosinoin); **d11**—benzyl dGSL (desulfoglucosinoin); **d48**—4-methoxyindol-3-ylmethyl dGSL (desulfo-4-methoxyglucobrassicin).

Author Contributions: Chemistry investigation: A.Đ., F.B. and I.B.; antiproliferative assays: V.Č.Č.; writing—original draft: A.Đ. and I.B.; writing—review and editing: all authors. All authors have read and agreed to the published version of the manuscript.

Funding: This research has been fully supported by the Croatian Science Foundation (Grant IP-2016-06-1316).

Institutional Review Board Statement: Not applicable.

Informed Consent Statement: Not applicable.

Data Availability Statement: The data presented in this study are available on request from the corresponding author. The data are not publicly available due to confidentiality agreements.

Acknowledgments: We are also thankful for the scientific-research equipment financed by the EU grant “Functional integration of the University of Split, PMF-ST, PFST, and KTFST through the development of the scientific and research infrastructure” (KK.01.1.1.02.0018).

Conflicts of Interest: The authors declare that they have no conflicts of interest.

References

1. Stevens, P.F. Angiosperm Phylogeny Website. Version 14. 2001. Available online: <http://www.mobot.org/MOBOT/research/APweb/> (accessed on 15 September 2023).
2. Gupta, S.K. *Biology and Breeding of Crucifers*; CRC Press, Taylor & Francis Group: New York, NY, USA, 2009.
3. Nikolić, T. (Ed.) *Flora Croatica Database*; Faculty of Science, University of Zagreb: Zagreb, Croatia, 2005; Available online: <http://hirc.botanic.hr/fcd> (accessed on 20 September 2023).
4. Çilden, E.; Özudoğru, B. Molecular phylogeny and phylogeography reveal recent divergence in the *Iberis simplex* DC. (*Brassicaceae*) species complex. *Turk. J. Bot.* **2022**, *46*, 567–582. [\[CrossRef\]](#)
5. Beilstein, M.A.; Al-Shehbaz, I.A.; Mathews, S.; Kellogg, E.A. Brassicaceae phylogeny inferred from phytochrome A and *ndhF* sequence data: Tribes and trichomes revisited. *Am. J. Bot.* **2008**, *95*, 1307–1327. [\[CrossRef\]](#)
6. Franzke, A.; Lysak, M.; Al-Shehbaz, I.A.; Koch, M.A.; Mummenhoff, K. Cabbage family affairs: The evolutionary history of Brassicaceae. *Trends Plant Sci.* **2011**, *16*, 108–116. [\[CrossRef\]](#) [\[PubMed\]](#)
7. Huang, C.H.; Sun, R.; Hu, Y.; Zeng, L.; Zhang, N.; Cai, L.; Zhang, Q.; Koch, M.A.; Al-Shehbaz, I.; Edger, P.P.; et al. Resolution of Brassicaceae phylogeny using nuclear genes uncovers nested radiations and supports convergent morphological evolution. *Mol. Biol. Evol.* **2015**, *33*, 394–412. [\[CrossRef\]](#) [\[PubMed\]](#)
8. Nikolov, L.A.; Shushkov, P.; Nevado, B.; Gan, X.; Al-Shehbaz, I.A.; Filatov, D.; Bailey, C.D.; Tsiantis, M. Resolving the backbone of the Brassicaceae phylogeny for investigation trait diversity. *New Phytol.* **2019**, *222*, 1638–1651. [\[CrossRef\]](#) [\[PubMed\]](#)

9. Hendriks, K.P.; Kiefer, C.; Al-Shehbaz, I.A.; Donovan Bailey, C.; van Huysduynen, A.H.; Nikolov, L.A.; Nauheimer, L.; Zuntini, A.R.; German, D.A.; Franzke, A.; et al. Global phylogeny of the Brassicaceae provides important insights into gene discordance. *bioRxiv* **2022**. [\[CrossRef\]](#)
10. Huang, X.C.; German, D.; Koch, M.A. Temporal patterns of diversification in *Brassicaceae* demonstrate decoupling of rate shifts and mesopolyploidization events. *Ann. Bot.* **2020**, *125*, 29–47. [\[CrossRef\]](#)
11. Edger, P.P.; Heide-Fischer, H.M.; Bekaert, M.; Rota, J.; Gloeckner, G.; Platts, A.E.; Heckel, D.; Der, J.P.; Wafula, E.K.; Tang, M.; et al. The butterfly plant arms-race escalated by gene and genome duplications. *Proc. Natl. Acad. Sci. USA* **2015**, *112*, 8362–8366. [\[CrossRef\]](#)
12. Edger, P.P.; Hall, J.C.; Harkess, A.; Tang, M.; Coombs, J.; Mohammadin, S.; Schranz, M.E.; Xiong, Z.; Leebens-Mack, J.; Meyers, B.C.; et al. *Brassicales* phylogeny inferred from 72 plastid genes: A reanalysis of the phylogenetic localization of two paleopolyploid events and origin of novel chemical defenses. *Am. J. Bot.* **2018**, *105*, 463–469. [\[CrossRef\]](#)
13. Agerbirk, N.; Hansen, C.C.; Kiefer, C.; Hauser, T.P.; Ørgaard, M.; Lange, C.B.A.; Cipollini, D.; Koch, M.A. Comparison of glucosinolate diversity in the crucifer tribe *Cardamineae* and the remaining order *Brassicales* highlights repetitive evolutionary loss and gain of biosynthetic steps. *Phytochemistry* **2021**, *185*, 112668. [\[CrossRef\]](#)
14. Đulović, A.; Popović, M.; Burčul, F.; Čikeš Čulić, V.; Marijan, S.; Ruščić, M.; Anđelković, N.; Blažević, I. Glucosinolates of *Sisymbrium officinale* and *S. orientale*. *Molecules* **2022**, *27*, 8431. [\[CrossRef\]](#) [\[PubMed\]](#)
15. Blažević, I.; Montaut, S.; Burčul, F.; Olsen, C.E.; Burow, M.; Rollin, P.; Agerbirk, N. Glucosinolate structural diversity, identification, chemical synthesis and metabolism in plants. *Phytochemistry* **2020**, *169*, 112100. [\[CrossRef\]](#) [\[PubMed\]](#)
16. Montaut, S.; Read, S.; Blažević, I.; Nuzillard, J.-M.; Roje, M.; Harakat, D.; Rollin, P. Investigation of the glucosinolates in *Hesperis matronalis* L. and *Hesperis laciniata* All.: Unveiling 4'-O-β-D-apiofuranosylglucosinolin. *Carbohydr. Res.* **2020**, *488*, 107898. [\[CrossRef\]](#) [\[PubMed\]](#)
17. Trabelcy, B.; Chinkov, N.; Samuni-Blank, M.; Merav, M.; Izhaki, I.; Carmeli, S.; Gerchman, Y. Investigation of glucosinolates in the desert plant *Ochradenus baccatus* (*Brassicales*: *Resedaceae*). Unveiling glucosinolin, a new arabinosylated glucosinolate. *Phytochemistry* **2021**, *187*, 112760. [\[CrossRef\]](#)
18. Schultz, O.E.; Gmelin, R. Das Senfölglykosid “Glukoiberin” und der Bitterstoff “Ibamarin” von *Iberis amara* L. (*Schleifenblume*). IX. Mitteilung über Senfölglykosid. *Arch. Pharm. Ber. Dtsch. Pharm. Ges.* **1954**, *287*, 404–411. [\[CrossRef\]](#) [\[PubMed\]](#)
19. Kjær, A.; Gmelin, R.; Larsen, I. isoThiocyanates. XII. 3-Methylthiopropyl isothiocyanate (ibervirin), a new naturally occurring mustard oil. *Acta Chem. Scand.* **1955**, *9*, 1143–1147. [\[CrossRef\]](#)
20. Bennett, R.N.; Mellon, F.A.; Kroon, P.A. Screening crucifer seeds as sources of specific intact glucosinolates using ion-pair high-performance liquid chromatography negative ion electrospray mass spectrometry. *J. Agric. Food Chem.* **2004**, *52*, 428–438. [\[CrossRef\]](#)
21. Mastelić, J.; Blažević, I.; Jerković, I. Free and bound sulphur containing and other volatile compounds from evergreen candytuft (*Iberis sempervirens* L.). *Croat. Chem. Acta* **2006**, *79*, 591–597.
22. Montaut, S.; Guido, B.S.; Grison, C.; Rollin, P. Identification of glucosinolates in seeds of three *Brassicaceae* species known to hyperaccumulate heavy metals. *Chem. Biodivers.* **2017**, *14*, e1600311. [\[CrossRef\]](#)
23. Mužek, M.N.; Omanović, D.; Đulović, A.; Burčul, F.; Svilović, S.; Blažević, I. The garden candytuft (*Iberis umbellata* L.): At the crossroad of copper accumulation and glucosinolates. *Processes* **2020**, *8*, 1116. [\[CrossRef\]](#)
24. Cole, R.A. Isothiocyanates, nitriles and thiocyanates as products of autolysis of glucosinolates in *Cruciferae*. *Phytochemistry* **1976**, *15*, 759–762. [\[CrossRef\]](#)
25. Danielak, R.; Borkowski, B. Biologically active compounds in seeds of crucifers Part III. Chromatographical search for glucosinolates. *Dissertationes Pharm. Pharmacol.* **1969**, *21*, 563–575.
26. Daxenbichler, M.E.; Spencer, G.F.; Carlson, D.G.; Rose, G.B.; Brinker, A.M.; Powell, R.G. Glucosinolate composition of seeds from 297 species of wild plants. *Phytochemistry* **1991**, *30*, 2623–2638. [\[CrossRef\]](#)
27. Kjær, A. isoThiocyanates XXXV. Miscellaneous isothiocyanate glucoside acetates. *Acta Chem. Scand.* **1959**, *13*, 851–852. [\[CrossRef\]](#)
28. Liu, X.-Y.; Ou, H.; Xiang, Z.-B.; Gregersen, H. Optimization, chemical constituents and bioactivity of essential oil from *Iberis amara* seeds extracted by ultrasound-assisted hydro-distillation compared to conventional techniques. *J. Appl. Res. Med. Aromat. Plants* **2019**, *13*, 100204. [\[CrossRef\]](#)
29. Weidner, C.; Rousseau, M.; Plauth, A.; Wowro, S.J.; Fischer, C.; Abdel-Aziz, H.; Sauer, S. *Iberis amara* extract induces intracellular formation of reactive oxygen species and inhibits colon cancer. *PLoS ONE* **2016**, *11*, e0152398. [\[CrossRef\]](#)
30. Clarke, D.B. Glucosinolates, structures and analysis in food. *Anal. Methods* **2010**, *2*, 310–325. [\[CrossRef\]](#)
31. Blažević, I.; Đulović, A.; Čikeš Čulić, V.; Popović, M.; Guillot, X.; Burčul, F.; Rollin, P. Microwave-assisted versus conventional isolation of glucosinolate degradation products from *Lunaria annua* L. and their cytotoxic activity. *Biomolecules* **2020**, *10*, 215. [\[CrossRef\]](#)
32. Al-Gendy, A.A.; Nematallah, K.A.; Zaghloul, S.S.; Ayoub, N.A. Glucosinolates profile, volatile constituents, antimicrobial, and cytotoxic activities of *Lobularia libyca*. *Pharm. Biol.* **2016**, *54*, 3257–3263. [\[CrossRef\]](#)
33. Agerbirk, N.; Hansen, C.C.; Olsen, C.E.; Kiefer, C.; Hauser, T.P.; Christensen, S.; Jensen, K.R.; Ørgaard, M.; Pattison, D.I.; Lange, C.B.A.; et al. Glucosinolate profiles and phylogeny in *Barbarea* compared to other tribe *Cardamineae* (*Brassicaceae*) and *Reseda* (*Resedaceae*), based on a library of ion trap HPLC-MS/MS data of reference desulfo-glucosinolates. *Phytochemistry* **2021**, *185*, 112658. [\[CrossRef\]](#)

34. Popović, M.; Maravić, A.; Čikeš Čulić, V.; Đulović, A.; Burčul, F.; Blažević, I. Biological effects of glucosinolate degradation products from horseradish: A horse that wins the race. *Biomolecules* **2020**, *10*, 343. [[CrossRef](#)] [[PubMed](#)]
35. Wang, N.; Wang, W.; Liu, C.; Jin, J.; Shaoa, B.; Shenc, L. Inhibition of growth and induction of apoptosis in A549 cells by compounds from oxheart cabbage extract. *J. Sci. Food Agric.* **2016**, *96*, 3813–3820. [[CrossRef](#)] [[PubMed](#)]

Disclaimer/Publisher’s Note: The statements, opinions and data contained in all publications are solely those of the individual author(s) and contributor(s) and not of MDPI and/or the editor(s). MDPI and/or the editor(s) disclaim responsibility for any injury to people or property resulting from any ideas, methods, instructions or products referred to in the content.